The Unification of Acceleration Envelope and Driveability Concepts

I.G. Salisbury, D.J.N. Limebeer, A. Tremlett and M. Massaro
Department of Engineering Science, University of Oxford, United Kingdom

ABSTRACT: The application of a frozen-time eigenvalue analysis to the straight line accelerating and braking of a race-car is presented. A three degree-of-freedom, single-track vehicle model is used to derive linear time-varying equations of motion. The response of the time-varying system is correlated with the frozen-time eigenvalues to predict the system stability. Theoretically, the use of eigenvalues to determine the stability of a time-varying system is only valid if the system is changing 'sufficiently slowly'. Bounds on the rate-of-change of the time-varying system are derived to determine the conditions under which this analysis is valid. Numerical evaluation of these bounds shows that the model studied can be classified as slowly-varying under accelerating and braking conditions, and is stable when the frozen-time eigenvalues are negative.

Keywords: G-G envelope, racing car, stability, controllability, driveability, motorsport

1 INTRODUCTION

Vehicle stability is frequently predicted using the frozen-time eigenvalues of a time-varying linearised model. In this type of analysis, the eigenvalues of a linearised vehicle model are computed at given speeds and longitudinal accelerations. If all the frozen-time eigenvalues have negative real parts, the vehicle is predicted, sometimes erroneously, to be stable. This approach was employed for motorcycle stability analysis in Limebeer et al. (2001) and Cossalter et al. (2008), and was applied more recently to the case of a race car in Tremlett et al. (2014).

The G-G diagram is a well-established representation of the vehicle performance envelope Brayshaw (2004); Milliken and Milliken (2005), allowing longitudinal and lateral acceleration limits to be described concisely for a given vehicle speed. The popularity of these diagrams stem from the clarity with which a large amount of information can be communicated. The effect on the performance envelope of changes in the vehicle parameters, or environment, can easily be visualised in this framework. Furthermore, by overlaying recorded telemetry data on a G-G plot, one can see the extent to which the driver is exploiting the car's performance envelope; an example of this is given in Figure 1. The vehicle's handling and stability characteristics influence the driver's ability to operate the vehicle on the depicted limit. In extreme cases an unstable vehicle can be undriveable, or negatively impact the driver's confidence. The highlighted regions in Figure 1 correspond to areas where the vehicle can be unstable and more difficult to drive. Consequently, it requires highly skilled drivers to drive the vehicle in these zones. Characterising the vehicle stability across the G-G diagram is a useful tool in assessing a vehicle and predicting the driveability of the vehicle at the limits of performance.

The treatment of stability over such a wide range of vehicle conditions has produced a number of approaches all with their limitations. Milliken and Milliken (2005) describe the use of stability and control derivatives to assist in the assessment of vehicle handling criteria, such as oversteer and understeer, Radt and Dis (1996). These derivatives are generated from linearised versions of the vehicle equations of motion at a steady-state operating point. Despite being practically useful and providing valuable insight into car behaviour, they only cover the portion of the G-G envelope relating to steady-state cornering conditions. Other, more sophisticated methods use phase plane

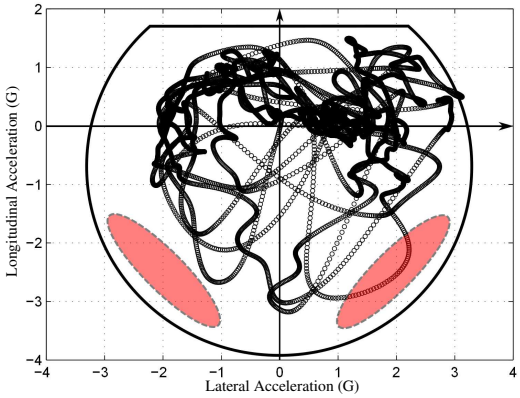

Figure 1. G-G diagram for a Formula 1 car qualifying at Silverstone.

and bifurcation analyses to determine vehicle stability Yi et al. (2012); these approaches are only suitable for use with simple vehicle models.

The frozen-time method addresses these problems, but one must be mindful of the fact that eigenvalues are not necessarily indicators of stability (or instability) in the case of linear time-varying systems Desoer (1969); Rosenbrock (1963). For that reason, a frozen-time eigenvalue analysis should be supported by simulation studies Limebeer et al. (2001); Cossalter et al. (2008).

The aim of the present work is to present a more rigorous assessment of frozen-time eigenvalue stability analysis and broaden the parts of the G-G diagram where it can be used.

This is achieved by computing a rate-of-change type bound for the linearised system eignevalues Desoer (1969); Rosenbrock (1963) and results are shown using a basic three degree-of-freedom car model with linear tyres. The stability in straight running is examined for both constant and accelerating conditions, and the results correlated with the response of the time-varying equations of motion. The bounds described in Rosenbrock (1963) are implemented with the vehicle model to determine the operating conditions under which the system is slowly time-varying and the eigenvalues truly indicative of stability. The mathematical vehicle model used in this work is presented in Section 2. The stability of the system is studied using the frozen time eigenvalue analysis in Section 3. In Section 4 the results are verified by determining analytically and numerically the conditions for stability. The conclusions and future work appear in Section 5.

2 VEHICLE MODEL

2.1 *Mathematical Model*

A simple bicycle model is used to describe the vehicle's dynamics and stability. The kinematics of the car model are shown in Figure 2, with all quantities described in an SAE coordinate system. Balancing forces in the longitudinal and lateral directions, and balancing yaw moments about the centre-of-mass gives the equations of motion (EOM):

$$m\dot{u} = m\omega v - F_{fy}\sin\delta + F_{rx} \quad (1)$$

$$m\dot{v} = -m\omega u + F_{fy}\cos\delta + F_{ry} \quad (2)$$

$$J\dot{\omega} = a\cos\delta F_{fy} - bF_{ry}. \quad (3)$$

The system states $x = [u, v, \omega]^T$ are the body-fixed longitudinal, lateral and yaw velocities. The parameters a, b, m and J represent the distance of the front and rear axle from the centre-of-mass, the mass of the vehicle and the vehicle yaw moment of inertia, respectively. The front wheel has steering angle δ. The front and rear lateral tyre forces are given by F_{fy} and F_{ry} respectively. The driven rear wheel has longitudinal tyre force F_{rx}. The side-slip angle β lies between the resultant vehicle velocity V and the vehicle's longitudinal axis. The front and rear tyre velocities make slip

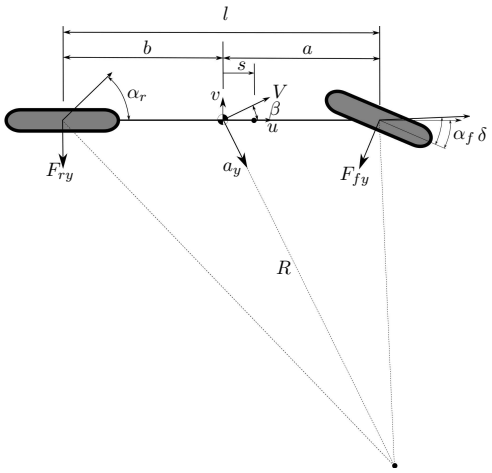

Figure 2. Kinematics of a single-track vehicle model showing the basic geometric parameters.

angles α_f and α_r with the wheel plane directions. These three angles are computed by:

$$\beta = \arctan(\frac{v}{u}), \tag{4}$$

$$\alpha_f = \arctan\left(\frac{u\sin\delta - \cos\delta(\omega a + v)}{u\cos\delta + \sin\delta(\omega a + v)}\right), \tag{5}$$

$$\alpha_r = \arctan\left(\frac{\omega b - v}{u}\right). \tag{6}$$

When the vehicle is accelerated, or braked, there is a normal tyre force transference between the front and rear axles. By balancing moments around the rear-wheel ground contact point, and noting the sum of the tyre down-forces is equal to the weight of the vehicle, the front and rear down-force, F_{fz} and F_{rz} respectively, can be computed as:

$$F_{fz} = mg - F_{rz}, \tag{7}$$

$$F_{rz} = mg\frac{a}{a+b} + ma_x\frac{h}{a+b}, \tag{8}$$

where, h is the height of the centre-of-mass and a_x is the longitudinal acceleration.

The lateral forces generated by the tyres are assumed to depend linearly on the tyre normal loads and slip angles, and are computed by:

$$F_{fy} = C_{f0}F_{fz}\left(\delta - \frac{\omega a + v}{u}\right), \tag{9}$$

$$F_{ry} = C_{r0}F_{rz}\left(\frac{\omega b - v}{u}\right), \tag{10}$$

where, C_{f0} and C_{r0} are the normalised cornering stiffnesses (at the front and rear axle), and (6) and (5) are simplified using small angle approximations.

Under straight-line conditions the influence of the mwv term on the longitudinal acceleration is assumed negligible, which decouples the longitudinal speed from the other two EOM. We will assume

$$u(t) = u_0 + a_x t. \tag{11}$$

The tyre model is combined with the remaining EOM, and under straight-line conditions the steady-state steering angle is zero. The resulting linear time-varying EOM are given by:

$$\dot{v} = -\frac{C}{mu(t)}v + \left(\frac{-Cs}{mu(t)} - u(t)\right)\omega, \tag{12}$$

$$\dot{\omega} = \frac{-Cs}{mk^2u(t)}v - \frac{Cq^2}{mk^2u(t)}\omega, \tag{13}$$

in which

$$C_r = C_{r0}F_{rz} \quad (14)$$
$$C_f = C_{f0}F_{fz} \quad (15)$$
$$Cs = C_f a - C_r b \quad (16)$$
$$C = C_f + C_r \quad (17)$$
$$Cq^2 = C_f a^2 + C_r b^2 \quad (18)$$
$$mk^2 = J. \quad (19)$$

Following Pacejka (2002), the parameter s is the distance from the centre-of-mass to the neutral steer point, q is the average moment arm and k the radius of gyration. The neutral steer point, which is shown in Figure 2, has kinematic significance; a force applied through this point will cause the vehicle to move laterally without changing the yaw angle.

The two first order differential equations in v and ω can be combined, and the lateral velocity eliminated, to get a second order differential equation in ω:

$$u(t)^2\ddot{\omega} + Pu(t)\dot{\omega} + (Qu(t)^2 + R)\omega = 0, \quad (20)$$

where, the values of the parameters P, Q and R are given by:

$$P = \frac{-k^2 m a_x + (a^2 + k^2)C_f + (b^2 + k^2)C_r}{mk^2}, \quad Q = -\frac{Cs}{mk^2}, \quad R = \frac{l^2 C_f C_r}{m^2 k^2}. \quad (21)$$

The closed-form solution of the time-varying equation is given by:

$$\omega = c_1 u^\rho(t) J_\nu(\alpha u(t)) + c_2 u^\rho(t) Y_\nu(\alpha u(t)), \quad (22)$$

where, J_v and Y_v are Bessel functions of the first and second kind, c_1 and c_2 are constants of integration, and the speed $u(t)$ is constrained by (11); see a similar analysis in Koiter and Pacejka (1968). The parameters ρ and α and the order of the Bessel functions ν are related to the coefficients of the differential equation by:

$$\rho = \frac{1 - \frac{P}{a_x}}{2}, \qquad \alpha = \sqrt{\frac{Q}{a_x^2}}, \qquad \nu = \sqrt{\frac{(1 - \frac{P}{a_x})^2}{4} - \frac{R}{a_x^2}}. \quad (23)$$

If the velocity is assumed constant, the equation reduces to a second order, time-invariant equation:

$$\ddot{\omega} + \frac{(a^2 + k^2)C_f + (b^2 + k^2)C_r}{mk^2 u_0}\dot{\omega} + \left(\frac{l^2 C_f C_r}{m^2 k^2 u_0^2} - \frac{Cs}{mk^2}\right)\omega = 0, \quad (24)$$

with the well-known solution given by:

$$\omega = c_1 e^{\lambda_1 t} + c_2 e^{\lambda_2 t}, \quad (25)$$

where, λ_1 and λ_2 are the eigenvalues of the system, and the constants c_1 and c_2 depend on the initial conditions.

3 VEHICLE STABILITY

3.1 *Steady-State Stability*

The stability of the constant-velocity version of the model given in Section 2.1 has been studied extensively, e.g. Pacejka (2002). Following the Routh-Hurwitz criterion, the system will be stable if all the coefficients in (24) are positive. With a linear tyre model all cornering stiffnesses are positive, hence only the last term in (24) can become negative, which occurs when the speed exceeds some critical value given by:

$$u_0 > V_{crit} = \sqrt{\frac{l^2 C_f C_r}{mCs}}. \quad (26)$$

The existence of a positive, real critical speed is dictated by the sign of the Cs term. Recalling equation (16), this depends on the location of the centre-of-mass and cornering stiffnesses of

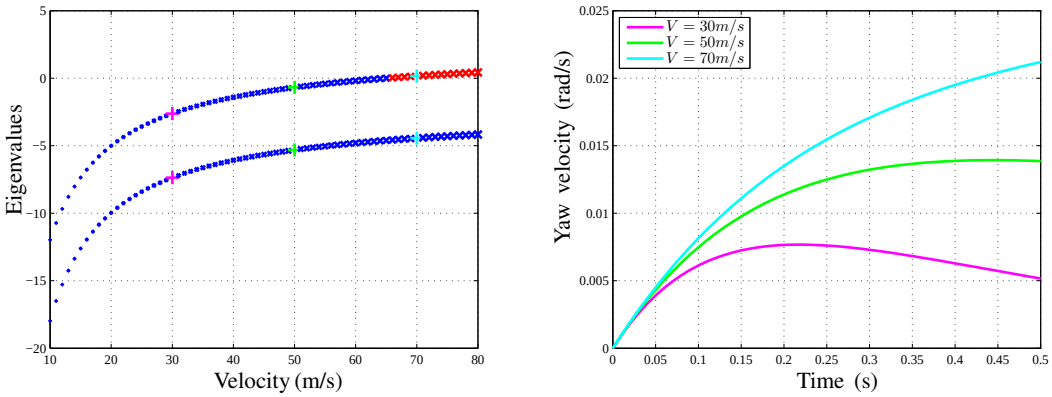

Figure 3. The left-hand figure shows the eigenvalues of the system for increasing vehicle speeds. Below the critical speed the eigenvalues are negative and the system is stable. The eigenvalues corresponding to the longitudinal speeds V_{ss} = {30m/s, 50 m/s, 70 m/s} are highlighted in green, cyan and magenta respectively. The right-hand figure contains the plots of the yaw response to a perturbation computed at the listed longitudinal speeds.

the tyres. This is linked to the concepts of over- and under-steer, which are usually described in the context of a cornering vehicle, Pacejka (2002). If a vehicle is negotiating a turn of constant radius, and the speed is increased, the steering angle required to maintain the turn will change. In an under-steering vehicle it will increase, in an over-steering vehicle it will decrease and in a neutrally steering vehicle it will remain constant. If Cs is positive the vehicle will over-steer and hence have a critical speed above which it is unstable. If, on the other hand, it is negative, the vehicle will under-steer and will not, at any speed, become unstable.

Table 1. Touring car vehicle parameters.

Parameter	Value
m	1200kg
l	2.7m
a	1.3m
b	1.4m
J	1700kg m^2

The stability of a touring car is studied, with the vehicle parameters given in Table 1. The tyre parameters are chosen in order to give an over-steering vehicle with a critical speed of $V_{crit} = 65m/s$. The two system eigenvalues are plotted in Figure 3 for vehicle speeds from $10m/s$ to $80m/s$. As the speed increases, the poles of the system can be seen to migrate towards the right-half plane, with one becoming positive when the critical speed is exceeded.

The eigenvalues at V = {30m/s, 50 m/s, 70 m/s} are highlighted and the response of the system to a perturbation in the initial yaw acceleration is determined at these speeds, and shown in the right half of Figure 3. At V = 30 m/s the system response exhibits stable behaviour, approaching a finite final value. At V=50 m/s the response is quicker, with the output achieving significantly larger values in the same time. At V=70 m/s the system is unstable and the response grows indefinitely.

3.2 *Frozen-time Eigenvalue Stability*

As a first step, the stability of the vehicle under braking and accelerating is studied by examining the eigenvalues of the frozen-time system (conventional approach). The vehicle is accelerated (or braked) and the frozen-time eigenvalues along the manoeuvre are computed. To verify the results, the poles are correlated with the time response of the yaw velocity to a perturbation.

The eigenvalues and system response at a constant -10 m/s^2 of braking are shown in Figure 4, for speeds from 80 to 10 m/s. One of the eigenvalues becomes positive at V_{crit} =23 m/s, much lower than the constant velocity case (65 m/s). The load transfer due to braking reduces the rear

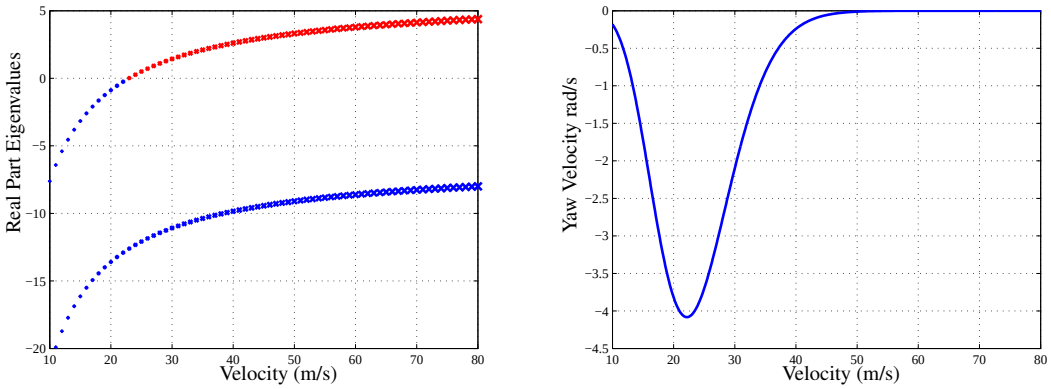

Figure 4. The left-hand figure contains a plot of the real part of the eigenvalues for a vehicle braking in straight line at -10 m/s^2 for vehicle speeds from 80 to 10 m/s. The right-hand figure contains the system time responses; the yaw velocity is perturbed at 10 m/s while the vehicle is braking.

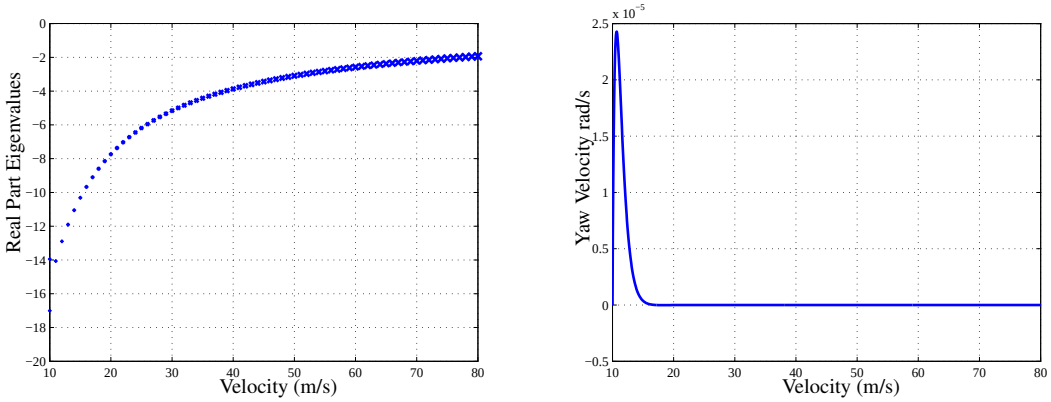

Figure 5. The left-hand figure contains a plot of the real part of the eigenvalues for a vehicle accelerating in straight line at 10 m/s^2 from 10 to 80 m/s. The right-hand figure contains the system time responses; the yaw velocity is perturbed at 10 m/s while the vehicle is accelerating.

tyre cornering stiffness, which causes Cs to increase, which, recalling (26), yields a lower critical speed. The response the time-varying system to a perturbation in yaw at 80 m/s is determined using the closed form solution in (22). Initially, the yaw angle grows exponentially, typical of an unstable system. However, as the vehicle speed decreases and the eigenvalues become negative, indicating stability, and the yaw response slows down, and then decays, returning to the initial state. This behaviour suggests that a vehicle braking from 80 m/s is not formally unstable, however, one may consider the presence of a large amplitude burst a practical instability. Nevertheless, by considering the migration of the eigenvalues in combination with the system response, the poles of the time-invariant system can be used to predict the stability of the time-varying system.

Under acceleration the eigenvalues of the system remain negative, and indeed, the system response to a perturbation exhibits a stable characteristic. At higher speeds the eigenvalues are complex, which manifests in an under-damped yaw response to a perturbation.

4 STABILITY OF LINEAR, TIME-VARYING SYSTEMS

In this section we aim to establish the conditions that allow the use of negative real eigenvalues of the frozen car model to infer the stability of the time varying (braking/accelerating) car model.

4.1 *Theory*

Rosenbrock (1963) and Desoer (1969) show that the time-varying linear system represented by:

$$\dot{x} = A(t)x, \tag{27}$$

is stable when the associated frozen-time eigenvalues are negative, and the rate of change of $A(t)$ is sufficiently slow. A detailed derivation of the upper bound on the rate of change of $A(t)$ used here is given in Rosenbrock (1963).

The time-varying matrix $A(t)$ is restricted to the form that corresponds to the differential equation:

$$x^n + a_n(t)x^{n-1} + ... + a_2(t)\dot{x} + a_1(t)x = 0, \tag{28}$$

where, x^n is the n^{th} derivative of x. The eigenvalues of $A(t)$ are uniquely related to the coefficients of the differential equation, and therefore bounds can be placed on the rates of change of the eigenvalues.

It is shown in Rosenbrock (1963) that if for all $t \geq t_0$, every $a_i(t)$ satisfies $|a_i| \leq a$ and is differentiable, and the eigenvalues λ of A are distinct and $Re(\lambda_i) \leq -\epsilon < 0$ for all i, then the point $x = 0$ is asymptotically stable if the matix $L(t)$ is negative definite for every $t \geq t_0$ and some $\eta > 0$, where

$$L = AS + SA^T - \dot{S} + \eta I, \tag{29}$$

and the matrix S is given by:

$$S_{ij} = \sum_{k=1}^{n} \lambda_k^{i-1} \bar{\lambda}_k^{j-1}. \tag{30}$$

4.2 *Application to Race-car*

The results of Rosenbrock (1963) are applied to the vehicle model for straight-line accelerating and braking conditions. The computation of the matrix S is simplified by considering the case of real and complex eigenvalues separately. Under braking the eigenvalues for the particular vehicle studied are real, and as a result of the load transfer to the rear, the eigenvalues are complex under accelerating. It is therefore convenient to study these two cases separately.

4.2.1 *Real Eigenvalues*

When the eigenvalues of $A(t)$ are real and the system second order, the matrix S is given simply by:

$$S(t) = \begin{bmatrix} 2 & -a_2 \\ -a_2 & a_2^2 - 2a_1 \end{bmatrix} \tag{31}$$

where, a_1 and a_2 are the coefficients of the differential equation (28).

The time-varying differential yaw equation in (20) can be rewritten in the form of (28), and, so S is found to be:

$$S(t) = \begin{bmatrix} 2 & -\frac{P}{u(t)} \\ -\frac{P}{u(t)} & \frac{P^2}{u^2(t)} - 2\left(Q + \frac{R}{u^2(t)}\right) \end{bmatrix}, \tag{32}$$

while $A(t)$ and $\dot{S}$ are given by:

$$A(t) = \begin{bmatrix} 0 & 1 \\ -\left(Q + \frac{R}{u^2(t)}\right) & -\frac{P}{u(t)} \end{bmatrix} \tag{33}$$

and,

$$\dot{S}(t) = \begin{bmatrix} 0 & \frac{Pa_x}{u^2(t)} \\ \frac{Pa_x}{u^2(t)} & \frac{4Ra_x - 2P^2a_x}{u^3(t)} \end{bmatrix}, \tag{34}$$

respectively.

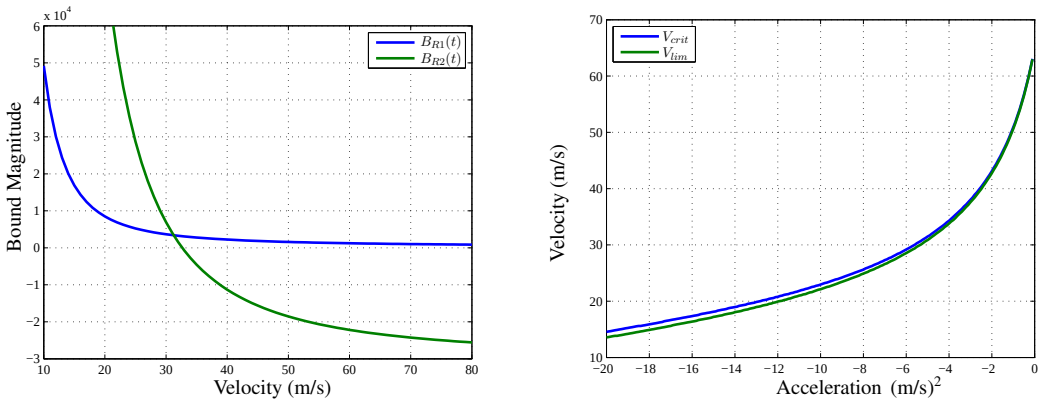

Figure 6. The left-hand plot contains the numerical evaluation of the bounds in (36) and (37) for vehicle speeds from 80 to 10 m/s, for a vehicle braking at -10 m/s^2. The right-hand plot shows the vehicle critical speed, and the limit speed as functions of the vehicle acceleration.

The matrix L can be determined analytically:

$$L(t) = \begin{bmatrix} -2\frac{P}{u(t)} & -\frac{-2P^2+Pa_x+4Qu^2(t)+4R}{u^2(t)} \\ -\frac{-2P^2+Pa_x+4Qu^2(t)+4R}{u^2(t)} & 2\frac{-P^3+P^2a_x+3PQu^2(t)+3PR-2Ra_x}{u^3(t)} \end{bmatrix} + \begin{bmatrix} \eta & 0 \\ 0 & \eta \end{bmatrix} \quad (35)$$

The requirement for stability is that L must be negative definite, which, since it is symmetric, implies its eigenvalues must be negative. From the Routh criterion, this requires that the coefficients of the characteristic polynomial be positive. These are determined analytically from L and with some rearranging are given by:

$$B_{R1}(t) = \frac{u^2(t)(P-3PQ)+P^3-P^2a_x+2Ra_x-3PR}{u^3(t)} > \eta > 0, \quad (36)$$

and,

$$B_{R2}(t) = \frac{-8Q^2u^4(t)+u^2(t)(2P^2Q-16QR-4PQa_x)+2P^2R-8R^2-\frac{1}{2}P^2a_x^2}{u^4(t)}$$
$$> -\eta^2+\eta\frac{u^2(t)(P-3PQ)+P^3-P^2a_x+2Ra_x-3RP}{u^3(t)} > 0, \quad (37)$$

where, the second condition has been simplified by assuming that the first condition holds. The time-varying vehicle system is stable when these two bounds are satisfied and the frozen-time eigenvalues are negative.

The conditions $B_{R1}(t)$ and $B_{R2}(t)$ in (36) and (37), respectively, are evaluated numerically for a vehicle braking at $-10m/s^2$ at speeds ranging from 80 to 10 m/s, with the results shown in the left plot of Figure 6. The first condition $B_{R1}(t) > 0$ always holds, but the second, $B_{R2}(t) > 0$, only holds below the limit speed V_{lim}=22.1 m/s.

In the frozen-time system the eigenvalues are negative below the vehicle critical speed V_{crit}. This speed is compared with V_{lim} for accelerations of -20 m/s^2 to 0 m/s^2 in right plot in Figure 6. At slower accelerations the critical and limit speeds are almost equal (being exactly equal at zero acceleration), but as the braking becomes stronger the limit speed becomes increasingly lower than the critical speed. This implies that the asymptotic stability of the time-varying system is assured for $u_0 < V_{lim}$, while the negative eigenvalues between V_{lim} and V_{crit} cannot be used to infer stability.

4.2.2 *Complex Eigenvalues*

When the system eigenvalues are complex, S is given by:

$$S = \begin{bmatrix} 2 & -a_2 \\ -a_2 & 2a_1 \end{bmatrix} = \begin{bmatrix} 2 & -\frac{P}{u(t)} \\ -\frac{P}{u(t)} & 2\left(Q+\frac{R}{u^2(t)}\right) \end{bmatrix}, \quad (38)$$

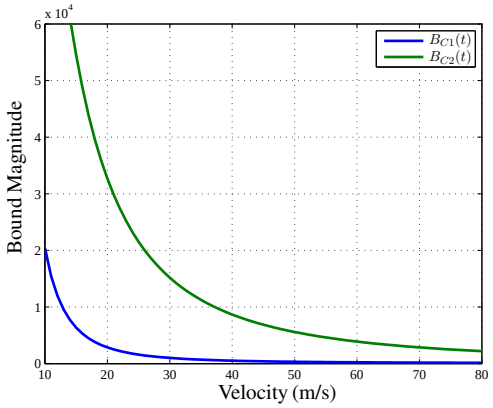

Figure 7. Numerical evaluation of conditions (40) and (41) for vehicle speeds between 10 and 80 m/s, with a vehicle accelerating at 10 m/s^2. Under accelerating conditions there is no critical speed.

and, thus L is found to be:

$$L(t) = \begin{bmatrix} -2\frac{P}{u(t)} & \frac{P^2 - Pa_x}{u^2(t)} \\ \frac{P^2 - Pa_x}{u^2(t)} & -2\frac{PQu^2(t) + PR - Ra_x}{u^3(t)} \end{bmatrix} + \begin{bmatrix} \eta & 0 \\ 0 & \eta \end{bmatrix}. \tag{39}$$

The sufficient conditions for stability are now given by:

$$B_{C1}(t) = \frac{u^2(t)(P + PQ) - Ra_x + PR}{u^3(t)} > \eta > 0, \tag{40}$$

and,

$$B_{C2}(t) = \frac{2P^2Qu^2(t) - 2PRa_x - \frac{1}{2}P^4 + 2P^2R + P^3a_x - \frac{1}{2}P^2a_x^2}{u^4(t)}$$
$$> -\eta^2 + \eta\frac{u^2(t)(P + PQ) - Ra_x + PR}{u^3(t)} > 0, \tag{41}$$

where, once again the second condition is simplified assuming the first is true.

The bounds $B_{C1}(t)$ and $B_{C2}(t)$ are evaluated for a vehicle accelerating at 10 m/s^2 and given in Figure 7. Across all vehicle speeds the bounds are satisfied, which implies that the system is asymptotically stable since the eigenvalues of the frozen-time system, as shown in Figure 5, are negative under acceleration.

5 CONCLUSION

While a frozen-time eigenvalue analysis can be used to study the stability of linear slowly time-varying systems, this technique must be used with caution. In most cases an alternative checking procedure, such as time simulations, or theoretically derived stability checks, should be used to verify the results. In the race-car context stability must be studied across the full performance envelope, and at large accelerations it is unclear whether an eigenvalue-based stability analysis is valid.

By applying the conditions derived in Rosenbrock (1963), it has been shown that the bounds given in (36), (37), (40) and (41) can be used to check the bicycle model stability up to some stability limit speed, which is generally lower than the critical speed given in (26). In the braking case, the classical critical speed is only slightly higher than the limit speed for accelerations up to 2G. In the accelerating case there is no classical critical speed, while the bounds (36), (37), (40) and (41) predict the vehicle model to be stable at high acceleration and high speed. These results support the notion that the system described by the simple bicycle model can be treated as slowly time-varying, and that the use of frozen-time eigenvalues to infer the stability in the straight-line accelerating and braking context is valid.

This analysis has clearly been conducted on a simple car model, which features linear tyres, where the load transfer of the vehicle is the dominant influence on the tyre cornering stiffnesses. The advantage of this approach, using a simple model, allows the car's stability to be determined analytically. The extent to which these conclusions extend to more complex vehicle models that incorporate complex tyre models, suspension systems, aerodynamic loads and so on remains to be investigated. In these cases, the L matrix may have to be computed numerically, although a symbolic evaluation may still be possible in some cases.

This work builds on established G-G diagram methods that are often favoured for their practicality, and the compact manner in which they convey critical information. Our work has extended the operating range over which G-G diagram and frozen-time type eigenvalue methods can be applied. Although the method is developed here using a simple vehicle model, it will hopefully remain applicable to higher fidelity models and a wider range of vehicle manoeuvres.

REFERENCES

Brayshaw, D. (2004). *The use of numerical optimisation to determine on-limit handling behaviour of race-cars*. PhD thesis, Department of Automotive, Mechanical and Structural Engineering, Cranfield University.

Cossalter, V., Lot, R., and Massaro, M. (2008). The chatter of racing motorcycles. *Vehicle Systems Dynamics*, 46(4):339–353.

Desoer, C. (1969). Slowly varying systems $\dot{x} = \mathrm{A}(t)x$. *IEEE Transactions on Automatic Control*, 14(12):780–781.

Koiter, W. and Pacejka, H. (1968). Skidding of vehicle due to locked wheels. *Proceedings of the Institute of Mechanical Engineers*, 183(8):3–18.

Limebeer, D., Sharp, R., and Evangelou, S. (2001). The stability of motorcycles under acceleration and braking. *Journal of Mechanical Engineeering Science*, 215(9):1095–1109.

Milliken, W. and Milliken, D. (2005). *Race car vehicle dynamics*. Warendale(PA) SAE.

Pacejka, H. (2002). *Tyre and Vehicle Dynamics*. Butterworth-Heinemann Ltd.

Radt, H. and Dis, D. V. (1996). Vehicle handling responses using stability derivatives. SAE Technical Paper 960483.

Rosenbrock, H. (1963). The stability of linear time-dependent control systems. *Journal of Electronic Control*, 15(1):73–80.

Tremlett, A., Assadian, F., Purdy, D., Vaughan, N., Moore, A., and Halley, M. (2014). Quasi-steady-state linearisation of the racing vehicle acceleration envelope: a limited slip differential example. *Vehicle Systems Dynamics*, 52(11):1416–1442.

Yi, J., Li, J., Lu, J., and Liu, Z. (2012). On the stability and agility of aggressive vehicle maneuvers: A pendulum-turn maneuver example. *IEEE Transactions on Control Systems Technology*, 20(3):663–676.